

Coordination of Tridentate Schiff Base Derivatives of 4-Aminoantipyrine to Rhenium (V)

Kim C. Potgieter¹, Thomas I.A. Gerber^{1,*} and Peter Mayer²

¹Department of Chemistry, Nelson Mandela Metropolitan University, 6031 Port Elizabeth, South Africa.

²Department of Chemistry, Ludwig-Maximilians University, D-81377, München, Germany.

Received 16 May 2011, revised 20 July 2011, accepted 11 November 2011.

Submitted by invitation to celebrate 2011 the 'International Year of Chemistry'.

ABSTRACT

The potentially tridentate Schiff base derivatives H₂nap and Hoap were synthesized by the condensation reaction of 4-amino-2,3-dimethyl-1-phenyl-5-pyrazoline (4-aminoantipyrine) with 2-aminobenzaldehyde and salicylaldehyde, respectively. The reaction of H₂nap with [ReOBr₃(PPh₃)₂] and *cis*-[ReO₂I(PPh₃)₂] (**1**) gives rise to the products [Re(nap)Br₂(PPh₃)₂]Br (**2**) and [ReO(OEt)(Hnap)(PPh₃)₂]I (**3**), respectively. In **2** the ligand nap is coordinated as a tridentate imido-imino-ketone, while in **3** Hnap is bonded as an amido-imino-ketone. The reaction of Hoap with [ReO₂I(PPh₃)₂] affords the product [ReO(OMe)(oap)(PPh₃)₂]I (**4**). Spectroscopic data and the X-ray crystal structures of compounds **2–4** are reported.

KEYWORDS

Tridentate, rhenium(V), imido, crystal structures.

1. Introduction

The research interest in pyrazolone (pz) and its derivatives is mainly due to their pharmaceutical properties. Pz is a five-membered lactam ring, containing two nitrogen atoms and a ketone, and it is an active moiety in pharmacology, such as for the treatment of arthritis and cancer, as analgesics, and as antiflammatory agents.¹ They have also found applications in catalysis,² analytical chemistry³ and solvent extraction.⁴

Due to the possible applications of the ^{186/188}Re radionuclides in radiotherapy, we studied the interaction of different oxorhenium(V) cores with derivatives of pyrazolone. The only atoms of pz available for coordination are the nitrogens of the pyrazole ring and the ketonic oxygen (Scheme 1). Blocking the nitrogen atoms by substitution, such as in antipyrine, only leaves the oxygen atom available for coordination. Transition metal complexes containing H₂aap have been extensively studied, with H₂aap coordinating as a bidentate neutral ligand in [M(H₂aap)₂X₂] (M=Co,Ni; X=Cl, SCN), or monodentately through the neutral amino nitrogen in [M(H₂aap)₄]Br₂ (M=Co, Ni).⁵

In this account the reactions of *trans*-[ReOBr₃(PPh₃)₂] and *cis*-[ReO₂I(PPh₃)₂] (**1**) with 4-(2-aminobenzylideneamino)-1,2-dihydro-2,3-dimethyl-1-phenylpyrazol-5-one (H₂nap) and

4-(2-hydroxybenzylideneamino)-1,2-dihydro-2,3-dimethyl-1-phenylpyrazol-5-one (Hoap; see Experimental section for structures) are reported, and the complexes *cis*-{Re(nap)Br₂(PPh₃)₂}Br (**2**), [ReO(OEt)(Hnap)(PPh₃)₂]I (**3**) and [ReO(OMe)(oap)(PPh₃)₂]I (**4**) were isolated and structurally characterized.

2. Experimental

2.1. Materials

All chemicals (Aldrich) were of reagent grade, and solvents were purified by standard techniques and drying methods. *Trans*-[ReOBr₃(PPh₃)₂] and *cis*-[ReO₂I(PPh₃)₂]⁶ were prepared by literature methods. H₂aap was purchased from Aldrich. All reactions and manipulations were carried out under nitrogen.

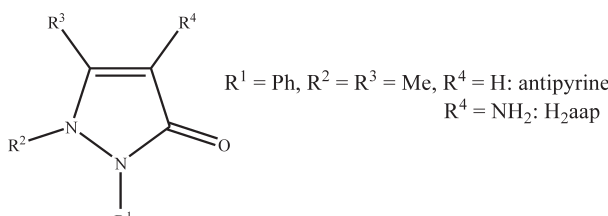
2.2. Physical Measurements

Infrared spectra were obtained with a Digilab FTS 3100 Excalibur HE spectrophotometer (SMM Instruments, Randburg, South Africa) with solid samples prepared as KBr disks. Microanalyses were obtained on a Carlo Erba EA 1108 elemental analyser (Waltham, MA, USA). Conductivity measurements (in the unit ohm⁻¹ cm² mol⁻¹) were done with 10⁻³ M solutions at 293 K with a Phillips PW 9509 conductometer (PANalytical, Randburg, South Africa). Electronic spectra were obtained with a Shimadzu UV-3100 spectrophotometer (ShimAnalytical, Roodepoort, South Africa), with λ_{max} reported in nm and extinction coefficients in M⁻¹ cm⁻¹.

2.3. Synthesis of the Ligands

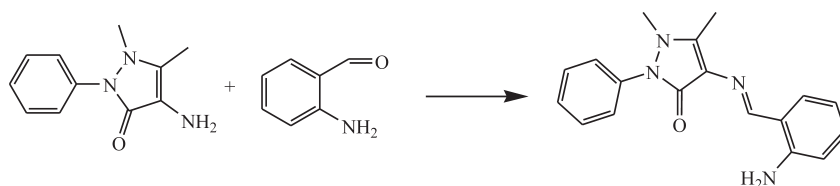
2.3.1. (4Z)-4-(2-aminobenzylideneamino)-1,2-dihydro-2,3-dimethyl-1-phenylpyrazol-5-one (H₂nap)

A solution of 0.840 g of 4-aminoantipyrine (4.13 mmol) in 20 cm³ of methanol was added dropwise to a solution of 0.505 g of 2-aminobenzaldehyde (4.17 mmol) in 30 cm³ of toluene, which



Scheme 1
Pyrazolone derivatives.

* To whom correspondence should be addressed. E-mail: thomas.gerber@nmmu.ac.za



was kept at -18°C (with a sludge bath of liquid nitrogen/1,2-dichlorobenzene). The reaction mixture was allowed to warm to room temperature, and then refluxed for three hours. On cooling the solution to room temperature, a yellow precipitate separated which was removed by filtration and dried under vacuum. Yield = 87 %, m.p. = 168°C . IR (cm^{-1}): $\nu(\text{N-H})$ 3039m, 3050m, $\nu(\text{C=O})$ 1646s, $\nu(\text{C=N})$ 1612 s. ^1H NMR (d_6 -DMSO; see Fig. 1 for labelling of hydrogen atoms): 9.62 (s, 1H, H₇), 7.52 (t, 2H, H₁₅, H₁₇), 7.36 (m, 3H, H₁₄, H₁₆, H₁₈), 7.23 (s, 2H, NH₂), 7.18 (d, 1H, H₂), 7.09 (t, 1H, H₃), 6.73 (d, 1H, H₅), 6.57 (t, 1H, H₄), 3.11 (s, 3H, C(12)H₃), 2.36 (s, 3H, C(11)H₃).

2.3.2. (4Z)-4-(2-hydroxybenzylideneamino)-1,2-dihydro-2,3-dimethyl-1-phenylpyrazol-5-one (Hoap)

A mass of 3.038 g of 4-aminoantipyrine (0.0149 mol) and 1.776 g of salicylaldehyde (0.145 mol) were dissolved in 50 cm³ of methanol. The resultant solution was heated to reflux under nitrogen for three hours to give a yellow solution, which was cooled to room temperature and filtered. The filtrate was placed in a cold room (0°C) overnight to produce yellow crystals, which was collected by filtration and dried under vacuum. Yield = 96 %, m.p. = 199°C . IR (cm^{-1}): $\nu(\text{C=O})$ 1653s, $\nu(\text{C=N})$ 1594s. ^1H NMR (d_6 -DMSO; see Fig. 3 for labelling of hydrogen atoms): 9.68 (s, 1H, H₇), 7.54 (t, 2H, H₁₅, H₁₇), 7.45 (d, 1H, H₁₆), 7.38 (m, 3H, H₁₄, H₁₈, H₅), 7.30 (t, 1H, H₃), 6.91 (m, 2H, H₂, H₄), 3.19 (s, 3H, C(12)H₃), 2.39 (s, 3H, C(11)H₃).

2.4. Synthesis of the Complexes

2.4.1. *cis*-[Re(nap)Br₂(PPh₃)₂]Br (2)

Solid *trans*-[ReOBr₃(PPh₃)₂] of mass 0.105 g (109 μmol) was added to a solution of 67 mg of H₂nap (219 μmol) in 20 cm³ ethanol, and the mixture was heated under reflux for 3 h. After cooling to room temperature, the solution was filtered and the filtrate was allowed to evaporate slowly at room temperature. After two days brown crystals were collected. Yield = 52 %, m.p. 192°C . Anal. Calc.: C, 43.6; H, 3.2; N, 5.6. Found: C, 43.8; H, 3.4; N, 5.6 %. IR (cm^{-1}): $\nu(\text{C=O})$ 1593 m, $\nu(\text{C=N})$ 1575s, $\nu(\text{Re=N})$ 1095 m, $\nu(\text{Re-O})$ 512 m, $\nu(\text{Re-N})$ 440 m. Conductivity (DMF): 83. UV-Vis(MeOH): 313 (10450), 370 (5110).

2.4.2. [ReO(OEt)(Hnap)(PPh₃)₂]I (3)

Solid *cis*-[ReO₂I(PPh₃)₂] of mass 0.104 g (120 μmol) and 0.072 g of H₂nap (235 μmol) were dissolved in 20 cm³ ethanol, and the mixture was heated under reflux for 3 h. After cooling to room temperature, the solution was filtered and the filtrate was left to evaporate at room temperature. After 3 days red crystals were collected, yield = 61 %, m.p. 183°C . Anal. Calc. for 3. $\frac{1}{2}\text{EtOH} \cdot \frac{1}{2}\text{H}_2\text{O}$: C, 48.1; H, 4.2; N, 6.6. Found: C, 48.2; H, 4.4; N, 6.8 %. IR (cm^{-1}): $\nu(\text{N-H})$ 3049 w, $\nu(\text{C=O})$ 1600s, 1578s, $\nu(\text{Re=O})$ 940 m, $\delta(\text{OCH}_2)$ 907 s, $\nu(\text{Re-O})$ 510 m, $\nu(\text{Re-NH})$ 440 m. Conductivity (MeOH): 116. UV-Vis (MeOH): 317 (13250), 370 (12300), 491 (420).

2.4.3. [ReO(OMe)(oap)(PPh₃)₂]I (4)

A mixture of 1 (102 mg, 117 μmol) and Hoap (73 mg, 237 μmol) in 20 cm³ of methanol was heated under reflux for 2 h. After

cooling to room temperature, the solution was filtered, and the filtrate was evaporated slowly, yielding brown crystals after 3 days. Recrystallization was from MeOH/CH₂Cl₂. Yield = 58 %, m.p. 179°C . Anal. Calc. for 4. CH₂Cl₂: C, 45.0; H, 3.6; N, 4.1. Found: C, 44.8; H, 3.8; N 4.4 %. IR (cm^{-1}): $\nu(\text{C=O})$ 1599 s, $\nu(\text{C=N})$ 1569 s, $\nu(\text{Re=O})$ 940s; $\nu(\text{Re-O})$ 530 m, 510 m. Conductivity (MeOH): 106. UV-Vis (MeOH): 316 (12400), 370 (12250), 481 (350).

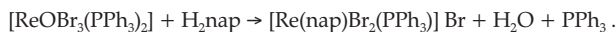
2.5. Crystallography

The X-ray diffraction studies were performed at 200(2) K using a Nonius Kappa CCD (for 2), and an Oxford Xcalibur (for 3 and 4) diffractometer with graphite monochromated Mo K α radiation ($\lambda = 0.71073 \text{ \AA}$). The structures were solved by direct methods applying SIR97⁷ and refined by least-squares procedures using SHELLXL-97⁸. All non-hydrogen atoms were refined anisotropically, and the hydrogen atoms were calculated in idealized geometrical positions (Table 1). The data were corrected by a numerical absorption correction⁹ after optimizing the crystal shape with XShape.¹⁰ In 2 the Br⁻ counter-ion is highly disordered, with a lot of remaining electron density present around it which could not be described properly. However, connectivity and other general features of the structure were confidently determined, and the molecular positional parameters of the atoms in the ‘inner core’ are well defined. In 3 the hydrogen atoms in the water molecule have not been considered in the refinement, with all the other hydrogens constrained. In 4 a split model has been applied to describe the disorder in N(2), N(3), C(13)–C(18). The sof ratio has refined to 0.66/0.34. Figure 3 shows the major part only.

3. Results

3.1. *cis*-[Re(nap)Br₂(PPh₃)₂] Br (2)

The reaction of a twofold molar excess of H₂nap with *trans*-[ReOBr₃(PPh₃)₂] in ethanol led to the formation of the six-coordinate rhenium (V) complex salt 2, according to the equation



The product is stable in air and in solution, and is soluble in polar solvents. It is a 1:1 electrolyte in DMF solution.

In the infrared spectrum a peak of medium intensity at 1095 cm⁻¹ is assigned to the Re=N(1) stretching frequency, with $\nu(\text{C}(8)=\text{O}(1))$ and $\nu(\text{C}(7)=\text{N}(2))$ of 1593 and 1575 cm⁻¹, respectively (see Fig. 2 for atom-numbering). There is no band in the 920–990 cm⁻¹ region that can be ascribed to $\nu(\text{Re=O})$.

An ORTEP perspective view of the complex cation is shown in Fig. 1. Due to the disorder of the bromide counter-ion, the structure could not be refined properly. The connectivity and other general features of the structure, however, were confidently determined, and the molecular positional parameters of the atoms in the ‘inner core’ are well defined. The rhenium atom is at the centre of a distorted octahedron. The basal plane can be defined by the three donor atoms of the nap chelate [the imido N(1), the imino N(2) and ketonic O(1)] and Br(1), with P(1) and Br(2) in *trans* axial positions. The distortion is mainly the result of

Table 1 Crystal and structure refinement data for the complexes.

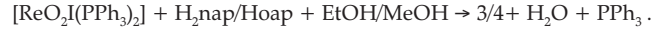
	2	3	4
Chemical formula	$C_{36}H_{31}N_4Br_3OPRe$	$C_{38}H_{37}IN_4O_3PRe \cdot \frac{1}{2}EtOH \cdot \frac{1}{2}H_2O$	$C_{38}H_{36}Cl_2IN_3O_4PRe$
Formula weight	992.60	973.85	1013.70
Crystal system	monoclinic	monoclinic	triclinic
Space group	$P2_1/c$	$P2_1/n$	$P-1$
a (Å)	18.4849(5)	18.1552(7)	8.9777(2)
b (Å)	15.7325(5)	10.5717(5)	14.8943(5)
c (Å)	13.6918(4)	20.1771(6)	16.3963(5)
α (°)			65.274(3)
β (°)	102.563(2)	96.620(5)	87.686(2)
γ (°)			74.037(2)
V (Å ³)	3886.4(2)	3846.8(3)	1907.7(1)
Z	4	4	2
D_{calc} (g cm ⁻³)	1.562	1.682	1.765
$F(000)$	1778	1908	988
μ (mm ⁻¹)	5.255	4.047	4.219
θ range (°)	3.2–25.4	4.2–26.3	4.2–26.4
Index ranges	−22/22, −18/17, −16/16	−16/22, −13/11, −22/25	11/11, −18/18, −20/20
Reflections measured	23596	18454	27595
Indpndt/obs reflections	7096/5723	7764/3976	7727/6249
Data/parameters	7096/415	7764/453	7727/419
Goodness-of-fit on F^2	1.954	0.80	1.09
Final R indices ($1 > 2\sigma(I)$)	0.0802/0.2476	0.0420/0.0833	0.0496/0.1049

a non-linear N(1)=Re-O(1) axis of 160.3(4)°, accomplished by Br(1)-Re-N(2) and Br(2)-Re-P(1) angles of 170.3(3)° and 171.53(9)°, respectively. The bite angles of nap are N(1)-Re-N(2) = 81.4(4)° and N(2)-Re-O(1) = 79.7(4)°. The nap ligand acts as a tridentate dianionic moiety, with N(1) coordinated as a dinegative imido nitrogen. The Re-N(1) bond length of 1.72(1) Å is considerably shorter than the values found for Re^V-NH and Re^V-NH₂ bonds [1.98–2.05 Å and 2.15–2.23 Å, respectively].^{11,12} The Re-N(1)-C(1) bond angle of 148(1)° indicates a significant deviation from linearity of the coordination mode of the phenylimido unit with a reduction in bond order of the Re=N(1) bond. The Re-N(2) length [2.15(1) Å] is typical of Re^V-N(imine)

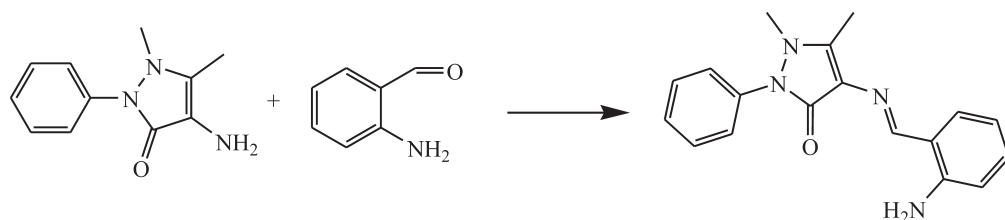
bonds.¹² The O(1)-C(8) bond length of 1.27(2) Å indicates a double bond, with the Re-O(1) length of 2.098(8) Å. The C(7)-N(2)-C(9) bond angle of 124(1)° is close to the ideal of 120° for a sp²-hybridized nitrogen atom, with the N(2)-C(7) bond double at 1.27(2) Å.

3.2. [ReO(OEt)(Hnap)(PPh₃)I] (3) and [ReO(OMe)(oap)(PPh₃)I] (4)

These complex salts were prepared by the reaction of *cis*-[ReO₂I(PPh₃)₂] with a twofold molar excess of H₂nap and Hoap, according to the equation

**Table 2** Selected bond lengths (Å) and angles (°) for complexes **2–4**.

	2	3	4
Re-N(1)	1.72(1)	Re-Br(1)	2.505(2)
Re-O(1)	2.098(8)	Re-Br(2)	2.560(1)
Re-N(2)	2.15(1)	Re-P(1)	2.422(3)
N(1)-Re-O(1)	160.3(4)	C(7)-N(2)-C(9)	124(1)
N(1)-Re-N(2)	81.4(4)	N(2)-Re-O(1)	9.7(4)
	3		
Re-O(2)	1.646(5)	Re-O(3)	1.877(4)
Re-O(1)	2.209(4)	Re-N(3)	2.155(5)
N(3)-C(12)	1.297(8)	Re-N(4)	1.979(6)
O(2)-Re-O(3)	165.0(2)	O(1)-Re-N(4)	169.4(2)
O(1)-Re-N(3)	80.4(2)	N(3)-Re-N(4)	90.2(2)
P(1)-Re-N(3)	174.9(2)	C(8)-N(3)-C(12)	126.6(6)
O(2)-Re-O(1)	84.9(2)	O(2)-Re-N(3)	91.8(2)
O(2)-Re-P(1)	93.2(1)	O(2)-Re-N(4)	100.3(2)
	4		
Re-O(3)	1.702(6)	Re-O(4)	1.886(5)
Re-O(1)	1.985(5)	Re-O(2)	2.171(7)
Re-N(1)	2.130(5)	N(1)-C(7)	1.296(8)
O(3)-Re-O(4)	168.5(2)	O(1)-Re-O(2)	170.9(2)
C(7)-N(1)-C(9)	126.5(6)	Re-O(4)-C(37)	147.1(5)
O(1)-Re-N(1)	92.3(2)	N(1)-Re-O(2)	80.5(2)
O(3)-Re-O(1)	98.8(2)	O(3)-Re-O(2)	87.5(3)
O(3)-Re-P(1)	91.7(2)	O(3)-Re-N(1)	96.3(2)



A single peak at 940 cm^{-1} in both the infrared spectra of **3** and **4** is assigned to the $\text{Re}=\text{O}$ stretching vibrations, with $\nu(\text{C}=\text{O})$ and $\nu(\text{C}=\text{N})$ at $1600/1599\text{ cm}^{-1}$ and $1578/1569\text{ cm}^{-1}$, respectively. The presence of the ethoxide is shown by an intense peak at 907 cm^{-1} , which corresponds to the ethoxy bending mode. The electronic spectra of **3** and **4** in methanol show two intense absorptions at about 315 and 370 nm , with a weaker one at around 485 nm . With reference to previous studies¹³ the band at highest energy is ascribed to a ligand-to-metal charge transfer transition [$\text{p}_\pi(\text{O}^2-) \rightarrow \text{d}_\pi^*(\text{Re})$], and the one at 370 nm to the $\text{p}_\pi(\text{O}(1) \rightarrow \text{d}_\pi^*(\text{Re})$ [$\text{d}_\pi^* = \text{d}_{xz}/\text{d}_{yz}$]. The weak absorption at lowest energy is probably due to a (d_{xy})² \rightarrow (d_{xy})¹(d_π^*)¹ transition.

The asymmetric unit of **3** contains half molecules of ethanol and water of crystallization. The molecular structure (Fig. 2) shows a distorted octahedral geometry around the Re(V) atom, with the equatorial plane formed by the $\text{P}(1)\text{O}(1)\text{N}(3)\text{N}(4)$ donor set, and the oxo $\text{O}(2)$ and $\text{O}(3)$ in *trans* axial positions. The *trans* angles $\text{O}(2)\text{-Re-O}(3)$ [$165.0(2)^\circ$] and $\text{O}(1)\text{-Re-N}(4)$ [$169.4(2)^\circ$] contribute significantly to the distortion, with $\text{P}(1)\text{-Re-N}(3)$ equal to $174.9(2)^\circ$. The $\text{N}(3)\text{-Re-N}(4)$ bite angle [$90.2(2)^\circ$], being part of a six-membered metallacycle, is considerably larger than the $\text{O}(1)\text{-Re-N}(3)$ one [$80.4(2)^\circ$]. The $\text{Re=O}(2)$ distance of $1.646(5)\text{ \AA}$ is shorter than for similar *trans* oxo-ethoxorhenium(V) complexes [average = $1.691(2)\text{ \AA}$].¹⁴ The $\text{Re O}(3)$ ethoxo bond [$1.877(4)\text{ \AA}$] is similar to similar bonds,¹⁵ but is substantially less than 2.04 \AA , which is considered to be representative of a $\text{Re}^{\text{V}}\text{-O}$ single bond.¹¹ Partial multiple bonding in $\text{Re-O}(3)$ is consistent with the

large $\text{Re-O}(3)\text{-C}(37)$ angle of $145.0(5)$. The $\text{O}(3)\text{-C}(37)$ length of $1.41(1)\text{ \AA}$ is normal for a single bond. The $\text{Re-N}(4)$ [$1.979(6)\text{ \AA}$] and $\text{Re-N}(3)$ [$2.155(5)\text{ \AA}$] bond lengths are typical for the coordination of amido and imino nitrogen atoms, respectively. The $\text{Re-O}(1)$ [$2.209(4)\text{ \AA}$] and $\text{O}(1)\text{-C}(7)$ [$1.278(8)\text{ \AA}$] lengths illustrate the rare coordination of a ketonic oxygen to rhenium(V).

The structure of **4** (Fig. 3) is very similar to that of **3**. The rhenium atom is displaced from the least-squares $\text{P}(1)\text{O}(1)\text{N}(1)\text{O}(2)$ plane towards the oxo oxygen atom $\text{O}(3)$. This displacement is the result of the non-orthogonal angles $\text{O}(3)\text{-Re-P}(1) = 91.7(2)^\circ$, $\text{O}(3)\text{-Re-O}(1) = 98.8(2)^\circ$, $\text{O}(3)\text{-Re-N}(1) = 96.3(2)^\circ$ and $\text{O}(3)\text{-Re-O}(2) = 87.5(3)^\circ$. This distortion results in a non-linear $\text{O}(3)\text{-Re-O}(4)$ axis of $168.5(2)^\circ$, with the $\text{Re=O}(3)$ distance [$1.702(6)\text{ \AA}$] significantly longer than in **3**. The $\text{Re-O}(4)$ length and $\text{Re-O}(4)\text{-C}(37)$ angle are $1.886(5)\text{ \AA}$ and $147.1(5)^\circ$, respectively, which are very similar to those values in **3**. In the tridentate oap chelate, $\text{O}(1)$ is monoanionic [$\text{Re-O}(1) = 1.985(5)\text{ \AA}$], $\text{N}(1)$ is an imino nitrogen [$\text{Re-N}(1) = 2.130(5)\text{ \AA}$, $\text{C}(7)\text{-N}(1)\text{-C}(9) = 126.5(6)^\circ$], and $\text{O}(2)$ is a neutral ketonic oxygen [$\text{C}(8)\text{-O}(2) = 1.27(1)\text{ \AA}$, $\text{Re-O}(2) = 2.171(7)\text{ \AA}$]. The $\text{O}(1)\text{-Re-N}(1)$ bite angle [$92.3(2)^\circ$] is larger than the corresponding angle in complex **3** [$90.2(2)^\circ$], with the $\text{N}(1)\text{-Re-O}(2)$ angle [$80.5(2)^\circ$] identical to that found in **3**.

4. Discussion

The ligand H_2nap gives rise to the formation of different types of products, depending on the starting complex. In its reaction

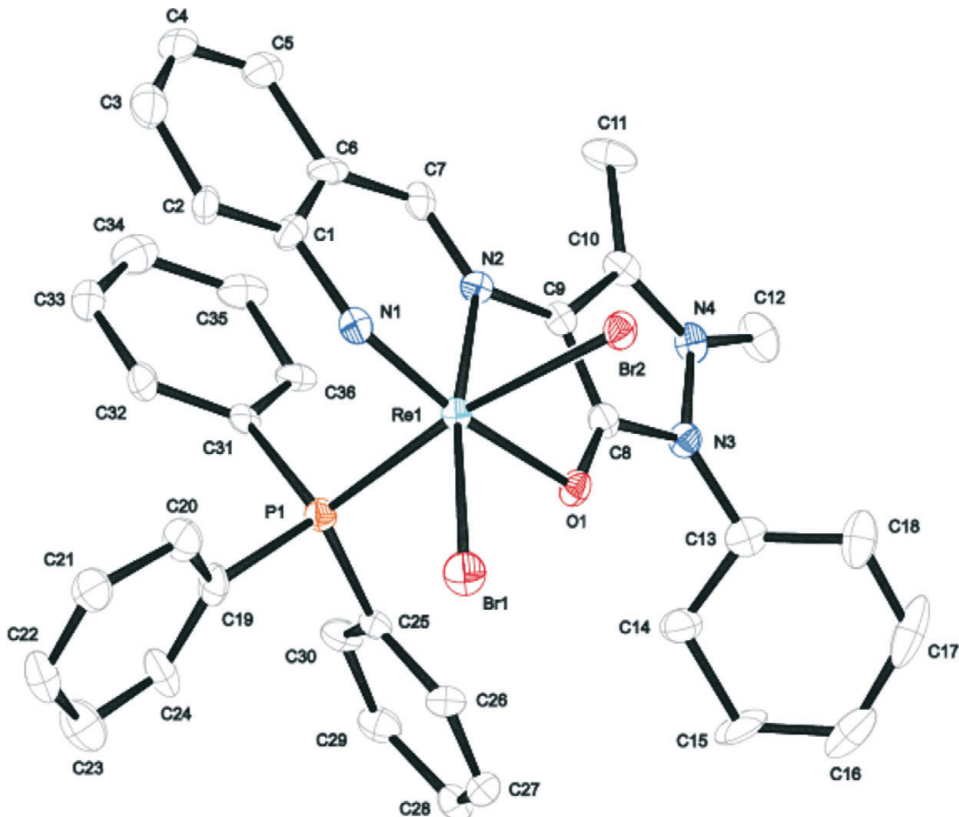


Figure 1 ORTEP plot of $[\text{Re}(\text{nap})\text{Br}_2(\text{PPh}_3)]^+$ (**2**), showing the atom-numbering. The bromide counter-ion and hydrogen atoms have been omitted.

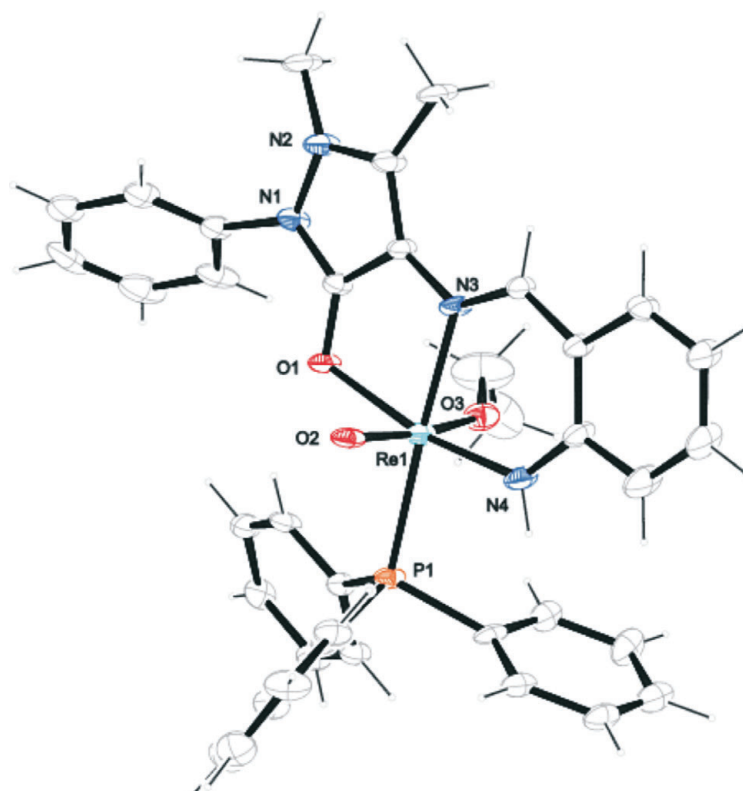


Figure 2 The structure of $[\text{ReO}(\text{OEt})(\text{Hnap})(\text{PPh}_3)]^+$. The counter-ion has been omitted.

with *trans*- $[\text{ReOBr}_3(\text{PPh}_3)_2]$, the complex salt $[\text{Re}(\text{nap})\text{Br}_2(\text{PPh}_3)]\text{Br}$ (2) is formed in which nap is coordinated as a tridentate dianionic imido-imino-ketone. With *cis*- $[\text{ReO}_2\text{I}(\text{PPh}_3)_2]$ the oxorhenium salt $[\text{ReO}(\text{OEt})(\text{Hnap})(\text{PPh}_3)]\text{I}$ (3) is produced, with Hnap present as a tridentate monoanionic amido-imino-ketone.

Although amido formation from phenylamino compounds with the oxorhenium core is common^{12–15} examples of rhenium(V) containing a tridentate imido-coordinated chelate have only been published recently.¹⁶

The reaction of Hoap with $[\text{ReO}_2\text{I}(\text{PPh}_3)_2]$ in methanol forms

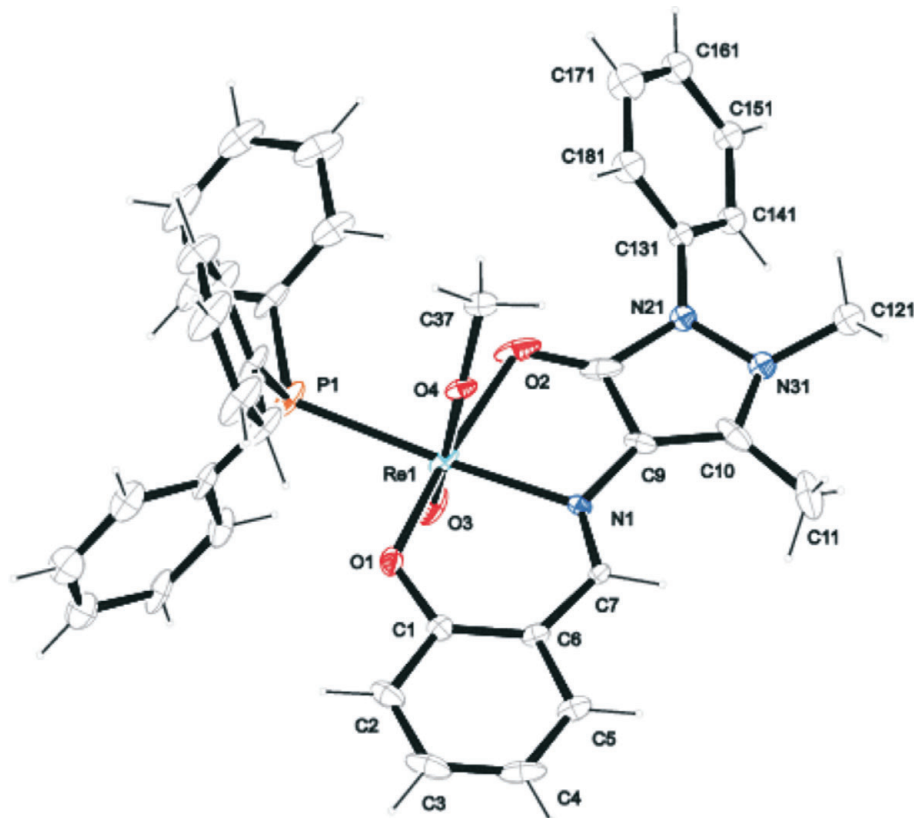


Figure 3 Perspective view and atom-labelling scheme for the molecular structure of $[\text{ReO}(\text{OMe})(\text{oap})(\text{PPh}_3)]^+$. The counter-ion has been omitted.

the salt $[\text{ReO}(\text{OMe})(\text{oap})(\text{PPh}_3)_3]\text{I}$ (**4**), in which oap is coordinated as a monoanionic phenoxy-imino-ketone. In oxorhenium(V) complexes containing tridentate Schiff base chelates with a phenolate oxygen, the phenolate oxygen usually occupies the site *trans* to the oxo group.¹⁷ In **4** the rigidity of the oap ligand probably prevents it from occupying one axial (*trans* to the oxo group) and two equatorial positions.

5. Conclusion

The products formed by the reactions of the Schiff base derivatives of 4-aminoantipyrine depend on the starting complex used. With the monooxorhenium(V) starting material $[\text{ReOBr}_3(\text{PPh}_3)_2]$, imido-coordination of the ligand occurs if a phenylamino group is present, as is shown in product **2**. However, with *cis*- $[\text{ReO}_2\text{I}(\text{PPh}_3)_2]$, one of the oxo groups is retained in the products, giving the complex salts **3** and **4**.

6. Supplementary Data

Files CCDC 818725 and 818726 contain the crystallographic data for complexes **3** and **4**, respectively. These data can be obtained free of charge at www.ccdc.cam.ac.uk/conts/retrieving/html, or from the Cambridge Crystallographic Data Centre (CCDC), 12 Union Road, Cambridge CB2 1EZ, UK; fax: +44(0)1223-336033; e-mail: deposit@ccdc.cam.ac.uk

References

- 1 A.P. Mishra, *J. Indian. Chem. Soc.*, 1999, **76**, 35–40; V. Cechiral Filho, R. Correa, Z. Vaz, J.B. Calixto, R.J. Nunes, T.R. Pinheiro, A.D. Andricopulo and R.A. Yunes, *Farmaco*, 1998, **53**, 55–57; R. Bose, D.S.R. Murty, G. Chakrapani, *J. Radioanal. Nucl. Chem.*, 2005, **265**, 115–122.
- 2 F. Bao, X. Lu, B. Kang and Q. Wu, *Eur. Polym. J.*, 2006, **42**, 928–934.
- 3 S.M. Sondhi, N. Shinghal, R.P. Verma, S.K. Arora and S.G. Dastidar, *Indian J. Chem.*, 2001, **B40**, 113–119.
- 4 T. Ito, C. Goto and K. Noguchi, *Anal. Chim. Acta*, 2001, **443**, 41–51.
- 5 R.A. Bailey and T.R. Peterson, *Can. J. Chem.*, 1969, **47**, 1681–1687.
- 6 N.P. Johnson, C.J.L. Lock and G. Wilkinson, *Inorg. Synth.*, 1967, **9**, 145–146; G.F. Ciani, G. D'Alfonso, P. Romiti, A. Sironi and M. Freni, *Inorg. Chim. Acta*, 1983, **72**, 29–37.
- 7 A. Altomare, M.C. Burla, M. Camalli, G.L. Gascarano, C. Giacavazzo, A. Guagliardi, A.G. Molterni, G. Polidori and R. Spagna, *J. Appl. Crystallogr.*, 1999, **32**, 115–117.
- 8 G.M. Sheldrick, *SHELXL-97, Program for Structure Solutions and Refinement*, University of Göttingen, Germany, 1997.
- 9 Xred, rev. 1.09, STOE, Darmstadt, Germany, 2005.
- 10 XShape, rev. 1.02, STOE, Darmstadt, Germany, 2005.
- 11 T.I.A. Gerber, D. Luzipo and P. Mayer, *J. Coord. Chem.*, 2004, **57**, 1419–1423.
- 12 T.I.A. Gerber, D. Luzipo and P. Mayer, *J. Coord. Chem.*, 2005, **58**, 637–641 (and references therein).
- 13 V.W.W. Yam, K.K. Tam, M.C. Cheng, S.M. Peng and Y. Wang, *J. Chem. Soc. Dalton Trans.*, 1992, 1717–1723; J.R. Winkler and H.B. Gray, *Inorg. Chem.* 1985, **24**, 346–355; V.W.W. Lam, Y.L. Pui, K.M.C. Wong and K.K. Cheung, *Inorg. Chim. Acta*, 2000, **300**, 721–732.
- 14 J.M. Mayer, *Inorg. Chem.*, 1988, **27**, 3899–3903.
- 15 T.I.A. Gerber and A. Abrahams, C. Imrie, P. Mayer, *J. Coord. Chem.*, 2004, **57**, 1339–1343.
- 16 I. Booyens, T.I.A. Gerber, E. Hosten, D. Luzipo and P. Mayer, *J. Coord. Chem.*, 2007, **60**, 635–640; I. Booyens, T.I.A. Gerber, E. Hosten and P. Mayer, *Bull. Chem. Soc. Eth.*, 2008, **22**, 101–105; P. Mayer, E. Hosten, T.I.A. Gerber and I. Booyens, *J. Iran. Chem. Soc.*, 2010, **7**, 775–780.
- 17 A. Abrahams, G. Bandoli, S. Gatto, T.I.A. Gerber and J.G.H. Du Preez, *J. Coord. Chem.*, 1998, **43**, 297–307; T.I.A. Gerber, P. Mayer and Z.R. Tshentu, *J. Coord. Chem.*, 2005, **58**, 1589–1595.